



# Angular Dependence of Fluctuation Conductivity in BaFe<sub>1.9</sub>Co<sub>0.1</sub>As<sub>2</sub> Single Crystal

M. Asiyaban<sup>1</sup> · S. R. Ghorbani<sup>2</sup> · S. N. Mirnia<sup>1</sup> · X. L. Wang<sup>3</sup>

Received: 25 March 2020 / Accepted: 11 April 2020  
© Springer Science+Business Media, LLC, part of Springer Nature 2020

## Abstract

Fluctuation conductivity of electron-doped BaFe<sub>1.9</sub>Co<sub>0.1</sub>As<sub>2</sub> single crystal is investigated by measurement of electrical resistivity under magnetic fields up to 13 T at different angles of  $\theta = 0, 45$  and  $90$  near mean-field transition temperature, where  $\theta$  is the angle between the applied magnetic field and the axis perpendicular to the  $ab$  plane. The mean-field transition temperature is determined using the peak of  $dR/dT$  curves. Using the Aslamazov–Larkin theory, four main regions are identified corresponding to 3D, 2D, 1D, and SW regions, respectively, for each angle at different magnetic fields. The 1D region is a sign of conducting charge strips that are believed that these 1D conducting strips might be responsible for the occurrence of high-temperature superconductivity. Anisotropy increases as it approaches  $T_c$ , suggesting unconventional superconductivity that might be due to multiband effects in crystal. Results show that the zero-temperature coherence length in the  $c$ -direction  $\xi(0)$ , the effective distance between the conducting layers  $d$ , and the channel cross section  $s$  decrease with increase in the magnetic field.

**Keywords** BaFe<sub>1.9</sub>Co<sub>0.1</sub>As<sub>2</sub> single crystal · Fluctuation conductivity · Dimensionality

## 1 Introduction

Many properties of a superconductor are changed as the temperature is reduced down to the critical temperature  $T_c$ , such as vanishing electrical resistivity, diamagnetism, and a jump in specific heat. Although such sharp distinction is reasonable for many experimental attempts, the introduction of superconducting fluctuations near superconducting transition has changed this idea. The apparent effect of superconducting fluctuations is rounding sharp corners and discontinuities occurring at  $T_c$  [1].

A wide variety of phenomena have been observed in the fluctuation regime, where in most cases the distribution of Cooper pairs due to creation and their annihilation changes when temperature decreases up to the vicinity of the critical

temperature  $T_c$ . The appearance of these short-life time particles above the  $T_c$  has some significant measurable effects on properties of superconductors above the superconducting transition temperature  $T_c$ . They influence the conductivity, the specific heat, the susceptibility [1], the magnetic relaxation rate, and the flux pinning [2,3]. Excess conductivity due to fluctuation is a potent tool to specify fundamental superconductor parameters such as the coherence length, the upper critical field,  $H_{c2}$ , and the dimensionality of transport, which are determined by measurement of physical quantities such as the magnetization and the resistivity.

Total fluctuation conductivity has different origins, and it is mainly due to a combination of three different effects:

$$\Delta\sigma^{fl} = \Delta\sigma^{AL} + \Delta\sigma^{MT} + \Delta\sigma^{DOS} \quad (1)$$

where  $\Delta\sigma^{AL}$  is the Aslamazov–Larkin (AL) term [4,5]. This term reflects the fact that the superconducting electron pairs contribute to the conduction above the critical temperature.  $\Delta\sigma^{MT}$  is the Maki–Thompson (MT) contribution [6,7], which is described as an influence of superconducting fluctuation on the normal quasiparticles.  $\Delta\sigma^{DOS}$  is the Density-of-States (DOS) contribution [8], which occurs because of the change in the density of normal-state carriers. The MT conductivity term is generally positive, like the AL term, while the DOS contribution has opposite signs compared with the AL

✉ S. R. Ghorbani  
sh.ghorbani@um.ac.ir

<sup>1</sup> Department of Physics, Faculty of Science, University of Mazandaran, Babolsar, Iran

<sup>2</sup> Department of Physics, Faculty of Science, Ferdowsi University of Mashhad, Mashhad, Iran

<sup>3</sup> Institute for Superconducting and Electronic Materials, University of Wollongong, Wollongong, NSW 2522, Australia

contribution. However, these contributions were small, and therefore, they are negligible in many experimental studies.

Above  $T_c$ , the creation and annihilation of Cooper pairs were induced by thermodynamic fluctuations. The formation of Cooper pairs results to an increase in electrical conductivity, which can be observed through the deviation of normal-state electrical resistivity at the fluctuation temperature of  $T_n$ . The excess conductivity was explained by Aslamazov–Larkin in the time-dependent Ginzburg–Landau framework (TDGL) [4,5]:

$$\Delta\sigma = \sigma - \sigma_n = 1/\rho^{-1}/\rho_n = A \varepsilon^{-\lambda} \tag{2}$$

where  $\rho$  and  $\rho_n$  are the measured electrical resistivity and the normal state electrical resistivity, respectively.  $\varepsilon = (T - T_c(H))/T_c(H)$  is the reduced temperature, and  $T_c(H)$  is the mean-field critical temperature at magnetic field of  $H$ .  $\lambda$  is equal to 0.5, 1, 1.5, and 3 for 3D, 2D, and 1D transport and short-wavelength fluctuation (SWF) regime, respectively, which depend on transport dimensionality.  $A$  is related to the dimensionality of transport, and it is given by

$$A = \begin{cases} \frac{e^2}{32\hbar\xi_c(0)} & \text{For 3D Fluctuations} \\ \frac{e^2}{16\hbar d} & \text{For 2D Fluctuations} \\ \frac{\pi e^2 \xi_c(0)}{16\hbar s} & \text{For 1D Fluctuations} \end{cases} \tag{3}$$

where  $\xi_c(0)$ ,  $d$ , and  $s$  are the coherence length at zero-temperature along the  $c$ -axis, the effective layer thickness of the 2D system, and the cross-section area of the 1D transport channel, respectively. As it can be seen in Eqs. (2) and (3), superconducting fluctuations are a potent tool to investigate superconductor properties such as dimensionality, which is a crucial point for potential applications [9].

In iron base superconductors, many experimental efforts have been made to study superconducting fluctuations [9–19] since their discovery in 2008 [20]. The analysis of hole-doped  $\text{Ba}_{0.72}\text{K}_{0.28}\text{Fe}_2\text{As}_2$  single crystal shows an MT-AL (3D–2D) crossover in fluctuations conductivity [19]. Experimental data indicate a decrease in the lifetime of fluctuation pairs by increasing the magnetic field. Superconducting fluctuations in  $\text{BaFe}_2(\text{As}_{0.68}\text{P}_{0.32})_2$  superconductors under the magnetic field up to 7 T show a 1D conducting channel in the superconductor [21]. This situation suggests that fluctuation superconductivity is present in a filamentary background formed by electron stripes. For a hole-doped  $\text{BaFe}_{2-x}\text{Ni}_x\text{As}_2$  superconductor with  $H_{c2}$  equal to 62 T, a 3D superconductivity is observed, while a 2D behavior is seen for F-doped of  $\text{LaOFeAs}$  with  $H_{c2} = 50$  T [18]. Measurement of electrical resistivity and magnetization of  $\text{BaFe}_2(\text{As}_{1-x}\text{P}_x)_2$  revealed multiband effects in this superconductor. Using Ullah–Dorsey scaling, K-doped  $\text{SrFe}_2\text{As}_2$

with  $\mu_0 dH_{c2}/dT \sim -4.2 \text{ T} \cdot \text{K}^{-1}$  shows a 3D behavior [9]. Scaling of the RFeAsO (R is the rare earth element) suggested a 3D–2D crossover of fluctuation conductivity [15].

The Ginzburg number ( $G_i$ ) shows the strength of the fluctuation effect.  $G_i$  defines as  $(8\pi^2 k_B T_c \lambda_{ab}^2 / \xi_c \Phi_0^2)^2 / 2$ , in which  $k_B$  is the Boltzman constant,  $\lambda_{ab}$  is the London penetration length parallel to the  $ab$  plane,  $\xi_c$  is the coherence length along the  $c$ -axis, and  $\Phi_0$  is the flux quantum [14]. For Fe-based superconductors,  $G_i$  is roughly  $10^{-4}$ , which is higher than the value of  $\text{MgB}_2$  with  $G_i \approx 10^{-6}$  [22] and lower than  $10^{-2}$  for cuprates [23,24]. Thus, observation of the fluctuation effect is expected in the conductivity of the Fe-based superconductors.

In [25], we analyzed the fluctuation conductivity as function of temperature in  $\text{BaFe}_{1.9}\text{Co}_{0.1}\text{As}_2$  single crystal for  $H \parallel c$ . However, the behavior of the fluctuation conductivity at the different applied magnetic field directions were not investigated.

In this paper, that is, in follow-up to earlier work [25], angular dependence of fluctuation conductivity is studied in electron-doped  $\text{BaFe}_{1.9}\text{Co}_{0.1}\text{As}_2$  single crystal under magnetic fields up to 13 T at different angles of  $\theta = 0, 45$ , and  $90$  near mean-field transition temperature, where  $\theta$  is the angle between the applied magnetic field and the axis perpendicular to  $ab$  plane ( $c$ -axis). Four main regions identified, which were corresponded to 3D, 2D, 1D, and SW regions, respectively, by using the Aslamazov–Larkin fluctuation theory for each angle at different magnetic fields. The 1D region is a sign of conducting charge strips that are believed that these 1D conducting strips might be responsible for the occurrence of high-temperature superconductivity.

## 2 Experimental Procedure

The  $\text{BaFe}_{1.9}\text{Co}_{0.1}\text{As}_2$  single crystal was prepared by the high-temperature self-flux method. Details of the single crystal growth are described elsewhere [14]. The as-grown single crystal cleaved and cut into a rectangular shape for measurements. The temperature dependence of the electrical resistivity was performed over the magnetic field range of 0–13 T with the applied current of 5 mA, using a physical property measurement system (PPMS, quantum design).

## 3 Results and Discussion

The temperature dependence of the electrical resistivity of  $\text{BaFe}_{1.9}\text{Co}_{0.1}\text{As}_2$  single crystal at a magnetic field range of 0–13 T for  $\theta = 0, 45$ , and  $90$  are shown in Fig. 1.  $\theta$  is the angle between the applied magnetic field and the  $c$ -axis.

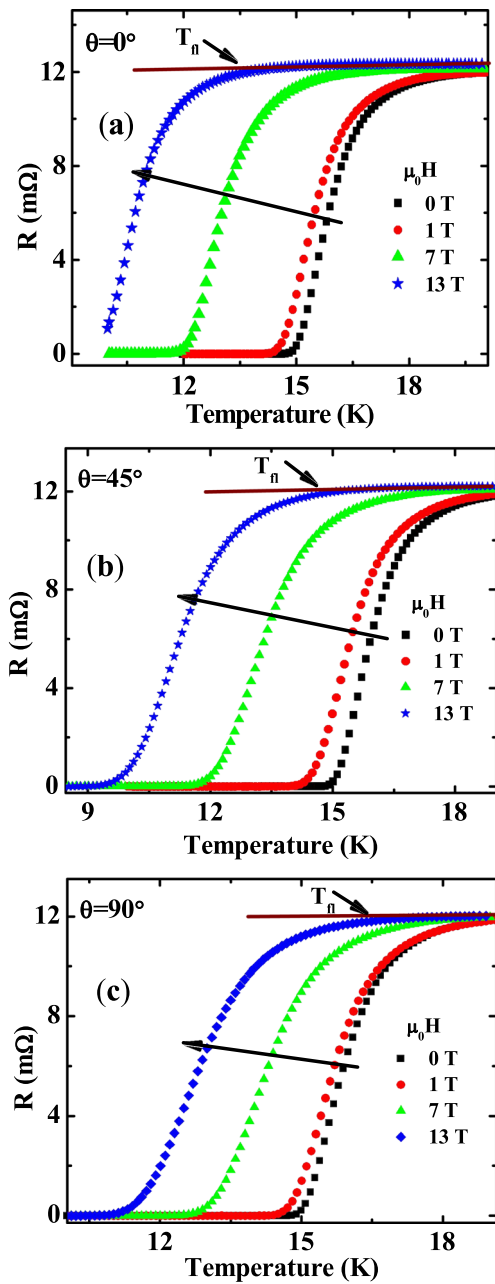


Fig. 1 Electrical resistivity vs. temperature at different applied magnetic fields for a  $\theta = 0$ , b 45, and c 90

For each angle, there is an evident displacement of resistive transition to lower temperatures by applying a magnetic field, which suggests a field-induced pair-breaking effect [26]. As it is seen in Fig. 1, broadening of resistive transition at  $\theta = 0$  is more significant than that for  $\theta = 90$ , which is due to higher activated vortex motion [27]. Results show that the transition from normal to the superconducting state for a magnetic field parallel to  $ab$  plane occurs at higher temperatures, indicating that the upper critical magnetic field in the  $ab$  plane  $H_{c2}^{ab}$  is higher than that the upper critical magnetic field in the  $c$ -axes direction  $H_{c2}^c$  [28].

Determining  $T_c(H)$  is a crucial parameter to evaluate excess conductivity. There are different criteria to determine the  $T_c(H)$ :  $\Delta\sigma^2(T)$  intercept with the temperature axis in  $\Delta\sigma^2 - T$  plot [19,29], the unique peak in the  $dR/dT$  curve [30–32], crossing point method [15,33], 50% of the normal-state electrical resistivity [34], 90% of the normal-state electrical resistivity [14], and temperature derivative of logarithm of  $\Delta\sigma$  [35]. Among these criteria, the peak of the  $dR/dT$  curve was generally used for determining  $T_c(H)$ . Therefore, this criterion is used here. Figure 2 shows the result of the  $T_c(H)$  for different angles. As is seen in Fig. 2,  $T_c(H)$  has a linear dependence concerning the applied magnetic field up to 13 for angles of 0, 45, and 90. It was found that the slope of the magnetic field,  $\mu_0 dH_{c2}/dT$ , with respect to temperature, which is shown in Fig. 3, decreases from  $\sim -2.53 \text{ T} \cdot \text{K}^{-1}$  to  $\sim -4.29 \text{ T} \cdot \text{K}^{-1}$  by increasing of angle from 0 to 90, respectively.

Anisotropy is defined as  $\gamma = \mu_0 H_{c2}^{ab} / \mu_0 H_{c2}^c = \mu_0 H_c(\theta = 90^\circ) / H_c(\theta = 0^\circ)$  [26], which is determined from 90% of the normal state resistance  $R_n(T_c)$  criteria in a different magnetic field. For  $T > 13 \text{ K}$ , the anisotropy of  $\text{BaFe}_{1.9}\text{Co}_{0.1}\text{As}_2$  single crystal is plotted in the inset of Fig. 3.  $\gamma$  increases as the temperature approaches  $T_c$ , in contrast to  $\text{SmFeAsO}_{0.8}\text{F}_{0.2}$  [36] and  $\text{MgB}_2$  [37], indicating unconventional superconductivity which might be due to multiband effects in the crystal [27] which is in agreement to Gasparov et al. [38].

It was found that the temperature dependence of the normal-state electrical resistivity at a temperature of  $T > T_{fl}$ , where  $T_{fl}$  is the fluctuation temperature, which can be expressed as  $R_n = R_0 + a T$ .  $R_0$  and  $a$  are the magnetic field dependence parameters.  $R_0$  is determined from extrapolating the electrical resistivity at temperature of 0 K, and  $a$  relates to the temperature coefficient of resistivity,  $\alpha = 1/R_0(\partial R/\partial T) = a/$

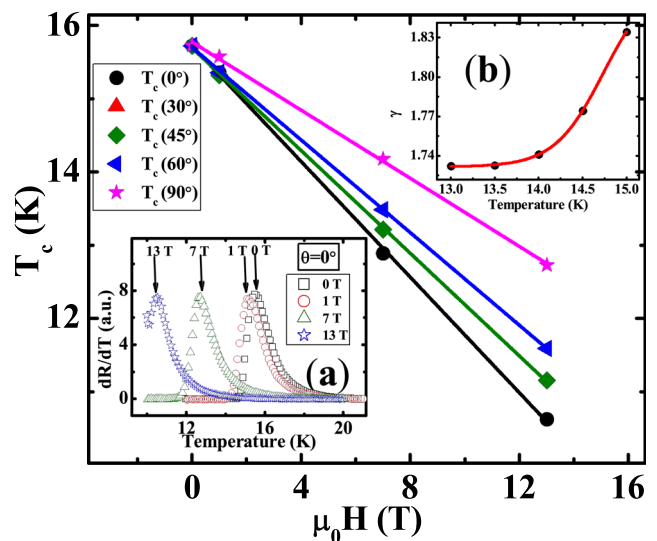


Fig. 2 The magnetic field dependence of  $T_c(H)$  at different angles. Inset: (a)  $dR/dT$  at a magnetic field of 0 T and 13 T for  $\theta = 0$ . (b) Temperature dependence of anisotropy. The red solid line guides to the eye

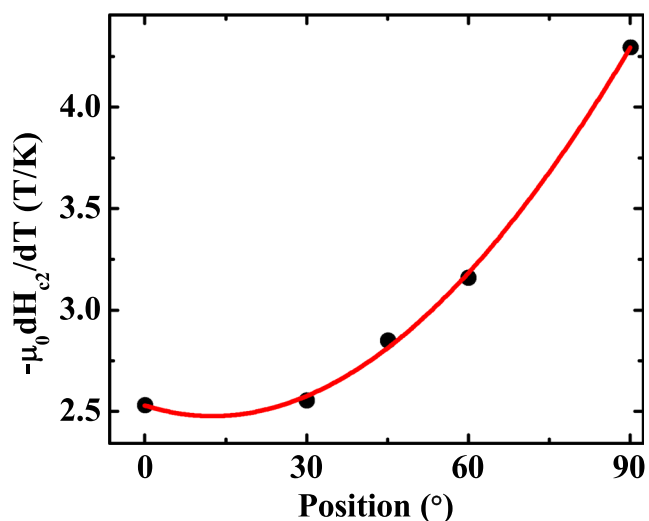


Fig. 3 Temperature dependence of  $\mu_0 dH_{c2}/dT$  at different angles

$R_0$ . Based on Homes' law,  $d\rho/dT$  is related to the London penetration depth  $\lambda_L$  [39], as  $d\rho/dT = (\mu_0 k_B / \hbar) \lambda_L^2$  [40].

Figure 4 shows the magnetic field dependence of  $R_0$  and  $a$ .  $R_0$  increments with an increasing magnetic field while  $a$  decrements. The variation of  $R_0$  becomes slower by increasing the angle between the magnetic field and the  $c$ -axis. For clarifying, the resistivity has been plotted as shown in Fig. 5 as a function of temperature at different angles for a magnetic field of 13 T at the vicinity of fluctuation temperature. Solid curves are the best fit of  $R_n = R_0 + a T$ . As it is shown in Fig. 5, for a magnetic field of 13 T, all fitted curves to the experimental data at temperature near the fluctuation temperature  $T_{fl}$  are parallel together for the angle smaller than 60 while there was a deviation from linearity for the  $\theta = 90$ . Based on the Homes' law, it means that the London penetration depth  $\lambda_L$  changed.

In Fig. 6, the reduced temperature  $\varepsilon$  dependence of the excess fluctuation conductivity  $\Delta\sigma$  in the magnetic field range

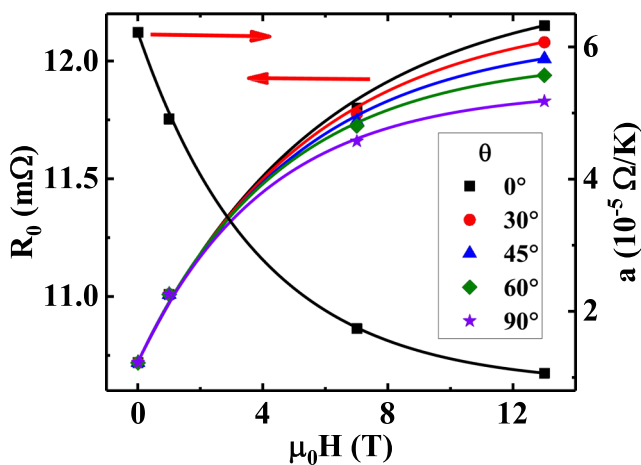


Fig. 4  $R_0$  and  $a$  parameters versus magnetic field at different angles. Solid lines are guides to the eye

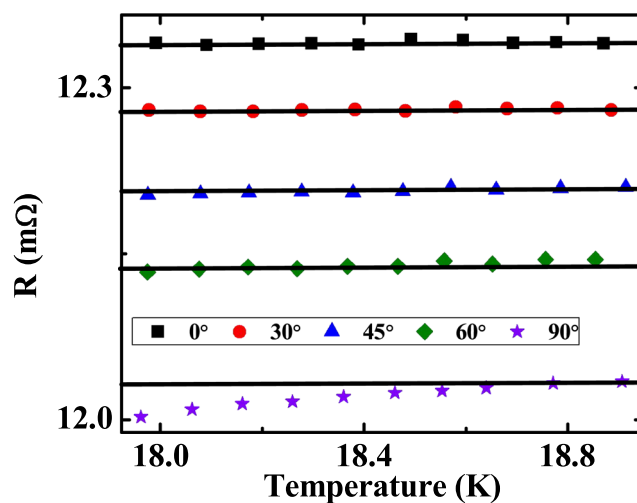


Fig. 5 Normal-state electrical resistivity near the fluctuation temperature  $T_{fl}$  at different angles in the magnetic field of 13 T

of 0–13 T are presented for  $\theta = 0, 45$ , and  $90$ . As is seen in Fig. 6, four different regions corresponding to different magnitudes of  $\lambda$  are specified. Near  $T_c(H)$ , there is 3D region corresponding to  $\lambda = 1/2$ , which is followed by 2D and 1D regions at higher temperatures with  $\lambda = 1$  and  $\lambda = 3/2$ , respectively. Also, there exists a short-wave fluctuation (SWF) region (much higher than the  $T_c(H)$ ), corresponding to  $\lambda = 3$ . Several granular superconductor materials with greatly anisotropic and inhomogeneous structures were found [41, 42] that the order parameter wavelength becomes comparable to the coherence length order in the SWF region, and therefore the Ginzburg–Landau (GL) theory breaks down [41].

The 1D filamentary fluctuation conductivity in electron-doped  $\text{BaFe}_{1.9}\text{Co}_{0.1}\text{As}_2$  single crystal is a sign of conducting charge strips, despite layered structure of Fe-based superconductors consisting of high-conductivity FeAs layers separated by low-conductivity layers. These conducting charge strips are considered as an electronic nematicity [43]. The charge stripes model includes magnetic and electronic structural characteristics, and the anti-ferromagnetic insulating zones separated segregation of charge inside domain walls. Despite the general belief of deleteriousness of magnetic ordering to superconductivity, some authors believe that these 1D conducting strips might be responsible for the occurrence of high-temperature superconductivity [44–46].

Arrows in Fig. 6 clearly show that the 3D–2D, 2D–1D, and 1D–SW transition crossovers at the temperatures of  $T_{3D \rightarrow 2D}$ ,  $T_{2D \rightarrow 1D}$ , and  $T_{1D \rightarrow SW}$ , respectively. Results of the transition crossovers temperatures are shown in Fig. 7 for both angles of 0 and 90. As it is seen in Fig. 7, the transition crossovers temperatures decrease linearly by increasing the applied magnetic field up to 13 T for both angles.

Figure 8 shows a comparison between the magnitudes of fluctuation conductivity as a function of reduced temperature at different angles for the magnetic field of 13 T. The inset of

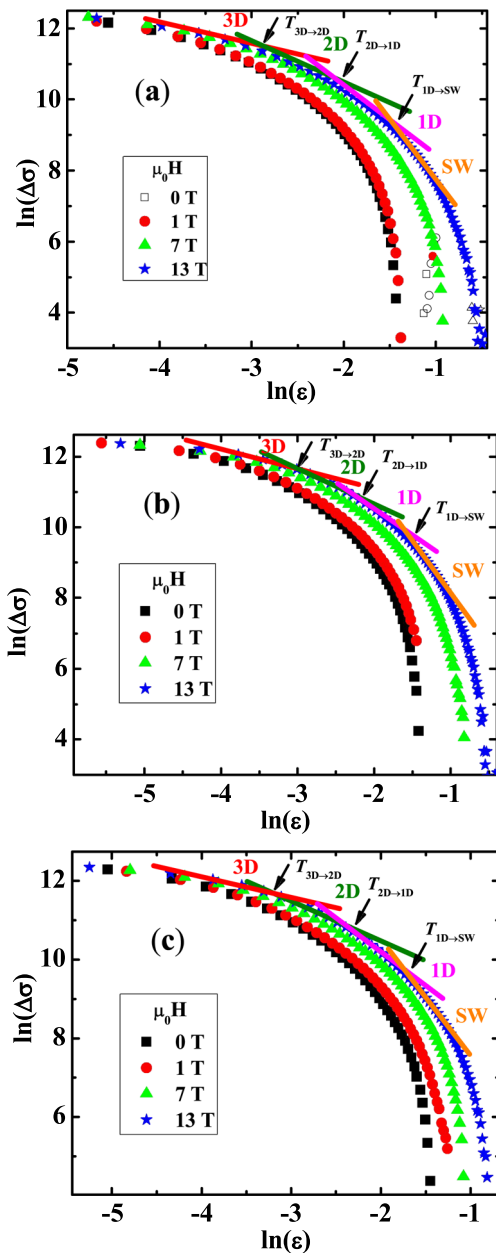


Fig. 6 The reduced temperature dependence of the excess fluctuation conductivity  $\Delta\sigma$  in a magnetic field of 0–13 T for **a**  $\theta=0$ , **b** 45, and **c** 90. Arrows show the crossover temperatures between different regions

Fig. 8 also shows the excess fluctuation conductivity versus temperature for clarifying. As it is seen in Fig. 8, there is no magnificent difference among the fluctuation conductivity versus the reduced temperature for different angles at 13 T since all experimental data collapse roughly into the one curve. At the same time, it depends on the mean-field critical temperature  $T_c$  (H), which was depended on the angle (see the inset of Fig. 8). The same trend is happened for other applied magnetic fields of 0, 1, and 7 T.

In order to the funding of well-established different regions, Eq. (2) in the mean-field region were fitted to the

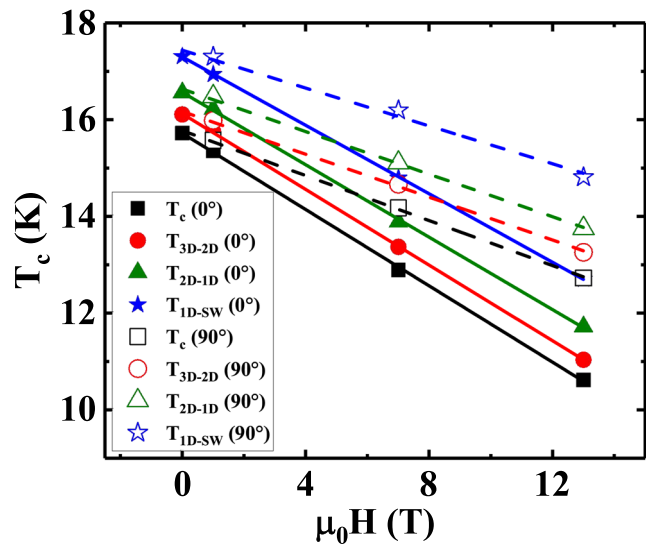


Fig. 7 Transition crossover temperatures for  $\theta=0$  and 90

experimental resistivity data at regions 3D, 2D, and 1D regions, corresponding to  $\lambda=0.5, 1,$  and  $1.5,$  respectively. By adjusting parameters of the  $\xi_c(0)$  in the 3D region, the  $d$  in the 2D region, and the  $s$  in the 1D region the best the theoretical curves of the electrical resistivity were found at different regions based on the AL contribution. Different colored curves illustrated results at a magnetic field of 13 T in Fig. 9 for the two angles of 0 and 90.

The fitting parameters of the  $d/\xi_c(0)$  ratio and the cross-section area of the channel in the 1D region,  $s$ , are illustrated in Fig. 10. As is seen in Fig. 10, both these parameters depend on the angles. The results show that both parameters reduce with increasing the magnetic fields while the variation of angle has a slight effect on them. These results suggested that the  $d$  decreases more than the  $\xi_c(0)$  with increasing the magnetic field. Filed dependence of the cross-section area of the

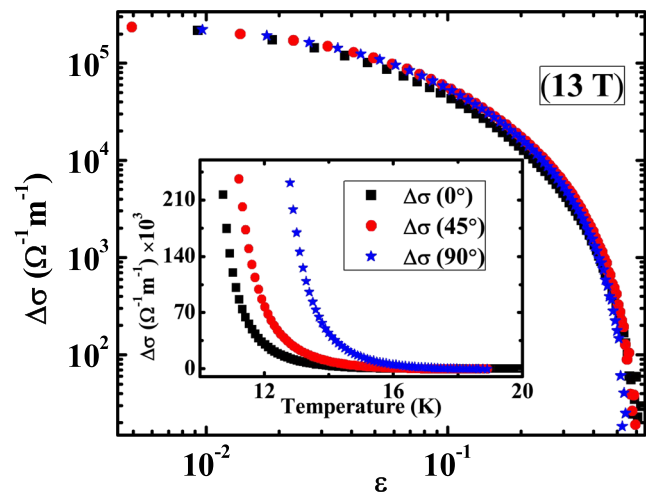
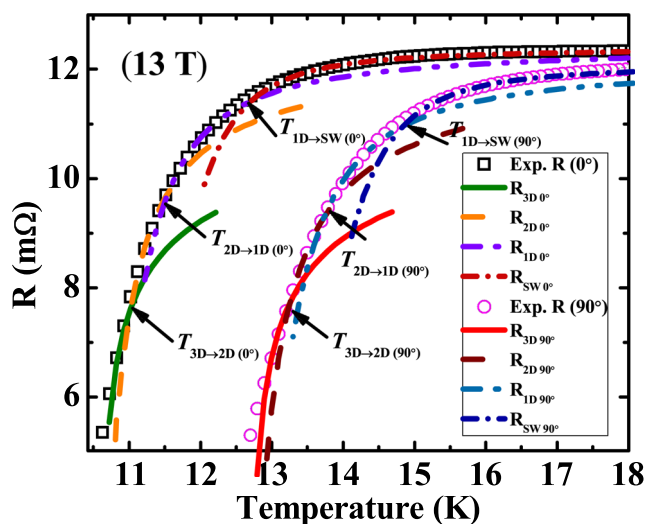


Fig. 8 Comparison of magnitudes of fluctuation conductivity at different angles for a magnetic field of 13 T



**Fig. 9** Temperature dependence of electrical resistivity at the 3D, 2D, 1D, and SWF regions for the magnetic field 13 T for different angles. Curves are fitting Eq. (3) to the experimental data of  $R$  at the 3D, 2D, 1D, and SWF regions. Arrows show the crossover temperatures in between different regions

channel,  $s$ , suggests that the one-dimensional structures are intrinsic features of its electronic properties [21].

### 4 Brief Conclusion

Fluctuation conductivity of electron-doped  $\text{BaFe}_{1.9}\text{Co}_{0.1}\text{As}_2$  single crystal is studied by measurement of electrical resistivity under magnetic fields up to 13 T at different angles of  $\theta = 0, 45, \text{ and } 90$  near mean-field transition temperature  $T_c$ , which is determined as a temperature in which a peak appears in  $dR/dT$  curves. Transition to the superconducting state for parallel magnetic field occurs at higher temperatures, indicating that

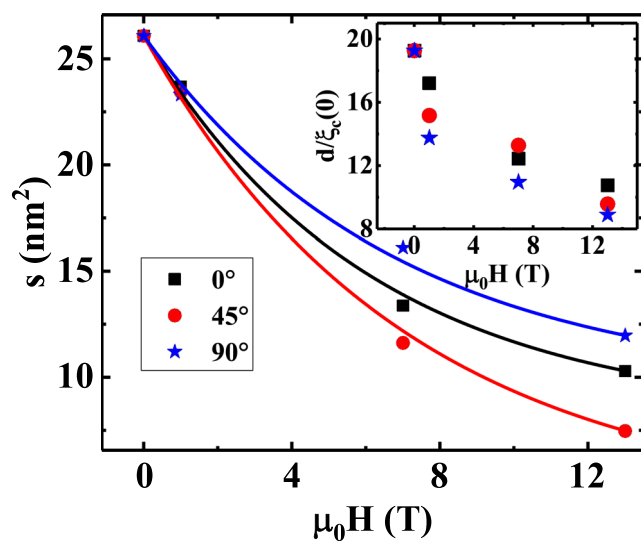


**Fig. 10** the  $d/\xi_c(0)$  ratio and the  $s$  versus the magnetic field for different angles. Solid lines are guides to the eye

$H_{c2}^{ab}$  is larger than  $H_{c2}^c$ . Using the Aslamazov–Larkin theory, four main regions are identified corresponding to 3D, 2D, 1D, and SW regions, respectively, for each angle at different magnetic fields. Results show that the 3D–2D, 2D–1D, and 1D–SW transition crossover temperatures of  $T_{3D \rightarrow 2D}$ ,  $T_{2D \rightarrow 1D}$ , and  $T_{1D \rightarrow SW}$ , respectively, have linear dependence concerning applied magnetic field up to 13 T. The 1D region is a sign of conducting charge strips which is believed that these 1D conducting strips might be responsible for occurrence of high-temperature superconductivity. Anisotropy increases as approaching  $T_c$ , suggesting unconventional superconductivity, which might be due to multiband effects in crystal. It was found that the zero-temperature coherence length in the  $c$ -direction  $\xi(0)$ , the effective distance between the conducting layers  $d$ , and the channel cross section  $s$  decrease with increasing the magnetic field.

### References

- Skocpol, W., Tinkham, M.: Fluctuations near superconducting phase transitions. Rep. Prog. Phys. **38**(9), 1049 (1975)
- Sang, L., Maheshwari, P., Liu, J., Li, Z., Qiu, W., Yang, G., Cai, C., Dou, S., Awana, V.S., Wang, X.: In-situ hydrostatic pressure induced significant suppression of magnetic relaxation and enhancement of flux pinning in  $\text{Fe}_{1-x}\text{Co}_x\text{Se}_{0.5}\text{Te}_{0.5}$  single crystals. Scr. Mater. **171**, 57–61 (2019)
- Shahbazi, M., Wang, X., Choi, K., Dou, S.: Flux pinning mechanism in  $\text{BaFe}_{1.9}\text{Ni}_{0.1}\text{As}_2$  single crystals: Evidence for fluctuation in mean free path induced pinning. Appl. Phys. Lett. **103**(3), 032605 (2013)
- Aslamazov, L.G., Larkin, A.I.: The influence of fluctuation pairing of electrons on the conductivity of normal metal. Phys. Lett. A. **26**(6), 238–239 (1968)
- Aslamazov, L., Larkin, A.: Effect of fluctuations on the properties of a superconductor at temperatures above the critical temperature. **10**, 1104–1111 (1968)
- Maki, K.: The critical fluctuation of the order parameter in type-II superconductors. Prog. Theor. Phys. **39**(4), 897–906 (1968)
- Thompson, R.S.: Microwave, flux flow, and fluctuation resistance of dirty type-II superconductors. Phys. Rev. B. **1**(1), 327–333 (1970)
- Varlamov, A., Balestrino, G., Milani, E., Livanov, D.: The role of density of states fluctuations in the normal state properties of high  $T_c$  superconductors. Adv. Phys. **48**(6), 655–783 (1999)
- Marra, P., Nigro, A., Li, Z., Chen, G., Wang, N., Luo, J., Noce, C.: Paraconductivity of the K-doped  $\text{SrFe}_2\text{As}_2$  superconductor. New J. Phys. **14**(4), 043001 (2012)
- Pallecchi, I., Fanciulli, C., Tropeano, M., Palenzona, A., Ferretti, M., Malagoli, A., Martinelli, A., Sheikin, I., Putti, M., Ferdeghini, C.: Upper critical field and fluctuation conductivity in the critical regime of doped  $\text{SmFeAsO}$ . Phys. Rev. B. **79**(10), 104515 (2009)
- Salem-Sugui, S., Ghivelder, L., Alvarenga, A.D., Pimentel, J.L., Luo, H., Wang, Z., Wen, H.-H.: Superconducting fluctuations in the reversible magnetization of the iron-pnictide  $\text{Ba}_{1-x}\text{K}_x\text{Fe}_2\text{As}_2$ . Phys. Rev. B. **80**(1), 014518 (2009)
- Solov'ev, A., Sidorov, S., Tarenkov, V.Y., D'yachenko, A.: Fluctuation conductivity and pseudogap in  $\text{SmFeAsO}_{1-x}$ . Low. Temp. Phys. **35**(10), 826–828 (2009)

13. Yamamoto, A., Jaroszynski, J., Tarantini, C., Balicas, L., Jiang, J., Gurevich, A., Larbalestier, D., Jin, R., Sefat, A., McGuire, M.A.: Small anisotropy, weak thermal fluctuations, and high field superconductivity in Co-doped iron pnictide  $\text{Ba}(\text{Fe}_{1-x}\text{Co}_x)_2\text{As}_2$ . *Appl. Phys. Lett.* **94**(6), 062511 (2009)
14. Kim, S.H., Choi, C.H., Jung, M.-H., Yoon, J.-B., Jo, Y.-H., Wang, X., Chen, X., Wang, X., Lee, S.-I., Choi, K.-Y.: Fluctuation conductivity of single-crystalline  $\text{BaFe}_{1.8}\text{Co}_{0.2}\text{As}_2$  in the critical region. *J. Appl. Phys.* **108**(6), 063916 (2010)
15. Liu, S.L., Haiyun, W., Gang, B.: Lowest Landau level scaling of the fluctuation conductivity for  $\text{RFeAsO}$  ( $\text{R}=\text{Nd, Pr, Sm}$ ) superconductors. *Phys. Lett. A.* **374**(34), 3529–3532 (2010)
16. Rullier-Albenque, F., Colson, D., Forget, A., Alloul, H.: Multiorbital effects on the transport and the superconducting fluctuations in  $\text{LiFeAs}$ . *Phys. Rev. Lett.* **109**(18), 187005 (2012)
17. Rey, R.I., Ramos-Álvarez, A., Carballeira, C., Mosqueira, J., Vidal, F., Salem-Sugui Jr., S., Alvarenga, A.D., Rui, Z., Huiqian, L.: Measurements of the superconducting fluctuations in optimally doped  $\text{BaFe}_{2-x}\text{Ni}_x\text{As}_2$  under high magnetic fields: probing the 3D-anisotropic Ginzburg–Landau approach. *Supercond. Sci. Technol.* **27**(7), 075001 (2014)
18. Wang, R., Li, D.-P.: Thermal fluctuation conductivity and dimensionality in iron-based superconductors. *Chin. Phys. B.* **25**(9), 097401 (2016)
19. Ghorbani, S.R., Wang, X.: In-field conductivity fluctuations in  $\text{Ba}_{0.72}\text{K}_{0.28}\text{Fe}_2\text{As}_2$  single crystals. *J. Supercond. Nov. Magn.* **1–5** (2017)
20. Kamihara, Y., Watanabe, T., Hirano, M., Hosono, H.: Iron-based layered superconductor  $\text{La}[\text{O}_{1-x}\text{F}_x]\text{FeAs}$  ( $x=0.05\text{--}0.12$ ) with  $T_c=26\text{ K}$ . *J. Am. Chem. Soc.* **130**(11), 3296–3297 (2008)
21. Costa, R.M., Alvarenga, A.D., Pureur, P.: Fluctuation conductivity in the presence of magnetic field and nematicity in the ferro-pnictide superconductor  $\text{BaFe}_2(\text{As}_{0.68}\text{P}_{0.32})_2$ . *Solid State Commun.* **288**, 74–78 (2019)
22. Kang, W., Kim, K.H., Kim, H.J.: Fluctuation of superconductivity in  $\text{MgB}_2$ . *J. Korean Phys. Soc.* **40**(5), 949–951 (2002)
23. Mun, M.-O., Lee, S., Bae, M.-K., Lee, S.-I.: Conductivity fluctuation in  $\text{HBCCO}$  superconductor. *Solid State Commun.* **90**(9), 603–606 (1994)
24. Mun, M.-O., Lee, S.-I., Lee, W.: Fluctuation magnetoconductance in  $\text{RNi}_2\text{B}_2\text{C}$  ( $\text{R}=\text{Y}$  and  $\text{Lu}$ ) single crystals. *Phys. Rev. B.* **56**(22), 14668 (1997)
25. Asiyaban, M., Ghorbani, S.R., Mirnia, S.N.: Fluctuation conductivity and its scaling behavior in  $\text{BaFe}_{1.9}\text{Co}_{0.1}\text{As}_2$  superconductor. *J. Supercond. Nov. Magn.* (2019). <https://doi.org/10.1007/s10948-019-05309-z>
26. Wang, Z.-S., Luo, H.-Q., Ren, C., Wen, H.-H.: Upper critical field, anisotropy, and superconducting properties of  $\text{Ba}_{1-x}\text{K}_x\text{Fe}_2\text{As}_2$  single crystals. *Phys. Rev. B.* **78**(14), 140501 (2008)
27. Wang, X.-L., Ghorbani, S.R., Lee, S.-I., Dou, S.X., Lin, C., Johansen, T., Müller, K.-H., Cheng, Z., Peleckis, G., Shabazi, M.: Very strong intrinsic flux pinning and vortex avalanches in  $(\text{Ba}, \text{K})\text{Fe}_2\text{As}_2$  superconducting single crystals. *Phys. Rev. B.* **82**(2), 024525 (2010)
28. Khim, S., Kim, J.W., Choi, E.S., Bang, Y., Nohara, M., Takagi, H., Kim, K.H.: Evidence for dominant Pauli paramagnetic effect in the upper critical field of single-crystalline  $\text{FeTe}_{0.6}\text{Se}_{0.4}$ . *Phys. Rev. B.* **81**(18), 184511 (2010)
29. Solovjov, A.L., Omelchenko, L.V., Terekhov, A.V., Rogacki, K., Vovk, R.V., Khlybov, E.P., Chroneos, A.: Fluctuation conductivity and possible pseudogap state in FeAs-based superconductor  $\text{EuFeAsO}_{0.85}\text{F}_{0.15}$ . *Mater. Res. Express.* **3**(7), 076001 (2016)
30. Chaudhary, S.: On the fluctuation induced excess conductivity in stainless steel sheathed  $\text{MgB}_2$  tapes. *J. Mater.* **2013**, (2013)
31. Khan, N.A., Hassan, N., Nawaz, S., Shabbir, B., Khan, S., Rizvi, A.A.: Effect of Sn substitution on the para-conductivity of polycrystalline  $\text{Cu}_{0.5}\text{Tl}_{0.5}\text{Ba}_2\text{Ca}_2\text{Cu}_{3-y}\text{Sn}_y\text{O}_{10-\delta}$  superconductors. *J. Appl. Phys.* **107**(8), 083910 (2010)
32. Ravi, S., Bai, V.S.: Fluctuation induced excess conductivity in the  $\text{Bi}_{1.2}\text{Pb}_{0.3}\text{Sr}_{1.5}\text{Ca}_2\text{Cu}_3\text{O}_y$  compound. *Phys. C. Supercond.* **182**(4–6), 345–350 (1991)
33. Moloni, K., Friesen, M., Li, S., Souw, V., Metcalf, P., Hou, L., McElfresh, M.: 3D XY and lowest Landau level fluctuations in deoxygenated  $\text{YBa}_2\text{Cu}_3\text{O}_{7.2d}$  thin films. *Phys. Rev. Lett.* **78**(16), 3173–3176 (1997)
34. Sónora, D., Carballeira, C., Ponte, J.J., Xie, T., Luo, H., Li, S., Mosqueira, J.: Quasi-two-dimensional behavior of 112-type iron-based superconductors. *Phys. Rev. B.* **96**(1), 014516 (2017)
35. Roa Rojas, J., Albino Aguiar, J., Landínez Téllez, D.: Conductivity fluctuations in the two-dimensional anisotropic  $\text{CaLaBaCu}_{3-x}\text{GaxO}_{7-\delta}$  superconductor. *Rev. Colomb. Fis.* **43**(3), 773 (2011)
36. Weyeneth, S., Puzniak, R., Mosele, U., Zhigadlo, N.D., Katrych, S., Bukowski, Z., Karpinski, J., Kohout, S., Roos, J., Keller, H.: Anisotropy of superconducting single crystal  $\text{SmFeAsO}_{0.8}\text{F}_{0.2}$  studied by torque magnetometry. *J. Supercond. Nov. Magn.* **22**(4), 325–329 (2009)
37. Angst, M., Puzniak, R., Wisniewski, A., Jun, J., Kazakov, S., Karpinski, J., Roos, J., Keller, H.: Temperature and field dependence of the anisotropy of  $\text{MgB}_2$ . *Phys Rev Lett.* **88**(16), 167004 (2002)
38. Gasparov, V.A., Drigo, L., Audouard, A., Sun, D., Lin, C., Bud'ko, S., Canfield, P., Wolff-Fabris, F., Wosnitzer, J.: Upper critical magnetic field in  $\text{Ba}_{0.68}\text{K}_{0.32}\text{Fe}_2\text{As}_2$  and  $\text{Ba}(\text{Fe}_{0.93}\text{Co}_{0.07})_2\text{As}_2$ . *JETP Lett.* **93**(11), 667 (2011)
39. Hu, T., Liu, Y., Xiao, H., Mu, G., Yang, Y.-F.: Universal linear-temperature resistivity: possible quantum diffusion transport in strongly correlated superconductors. *Sci Rep.* **7**(1), 9469 (2017)
40. Homes, C., Dordevic, S., Bonn, D., Liang, R., Hardy, W., Timusk, T.: Coherence, incoherence, and scaling along the  $c$  axis of  $\text{YBa}_2\text{Cu}_3\text{O}_{6+x}$ . *Phys Rev B.* **71**(18), 184515 (2005)
41. Cimberle, M., Ferdeghini, C., Giannini, E., Marre, D., Putti, M., Siri, A., Federici, F., Varlamov, A.: Crossover between Aslamazov-Larkin and short-wavelength fluctuation regimes in high-temperature-superconductor conductivity experiments. *Phys. Rev. B.* **55**(22), R14745 (1997)
42. Al-Otaibi, A., Almessiere, M., Salem, M.B., Azzouz, F.B.: Excess conductivity analysis in  $\text{YBa}_2\text{Cu}_3\text{O}_{7-d}$  added with  $\text{SiO}_2$  nanoparticles and nanowires: comparative study. *Mod. Phys. Lett. B.* **30**(20), 1650242 (2016)
43. Ando, Y., Segawa, K., Komiya, S., Lavrov, A.: Electrical resistivity anisotropy from self-organized one dimensionality in high-temperature superconductors. *Phys. Rev. Lett.* **88**(13), 137005 (2002)
44. Carlson, E., Orgad, D., Kivelson, S., Emery, V.: Dimensional crossover in quasi-one-dimensional and high-T  $C$  superconductors. *Phys. Rev. B.* **62**(5), 3422 (2000)
45. Kivelson, S.A., Fradkin, E., Emery, V.J.: Electronic liquid-crystal phases of a doped Mott insulator. *Nature.* **393**(6685), 550 (1998)
46. Emery, V., Kivelson, S., Zachar, O.: Spin-gap proximity effect mechanism of high-temperature superconductivity. *Phys. Rev. B.* **56**(10), 6120 (1997)